International Journal of Navigation and Port Research
Vol.29, No.7 pp. 627~634, 2005 (ISSN-1598-7701)

Analysis of Numerical Model Wave Predictions for Coastal Waters at Gunsan-Janghang Harbor Entrance

Joong-Woo Lee · Hak-Seung Lee** · Hoon Lee*** · Min-Su Jeon**** · Kang-Min Kim******

** Division of Civil and Environmental System Engineering, Korea Maritime University, Busan 606-791, Korea*
*** Ulsan New Container Terminal Corporation*
**** Graduate school of Korea Maritime University, Busan 606-791, Korea*
***** Undergraduate school of Korea Maritime University, Busan 606-791, Korea*
****** Seil Engineering Co., Ltd. Port and Coastal Development Institute, Seoul 150-051, Korea*

Abstract : *Gunsan-Janghang Harbor is located at the mouth of Gum River, on the central west coast of Korea. The harbor and coastal boundaries are protected from the effects of the open ocean by natural coastal islands and shoals due to depositions from the river, and two breakwaters. The navigation channel commences at the gap formed by the outer breakwater and extends through a bay via a long channel formed by an isolated jetty. For better understanding and analysis of wave transformation process where a wide coastline changes appear due to on-going reclamation works, we applied the spectral wave model including wind effect to the related site, together with the energy balance models. This paper summarizes comparisons of coastal responses predicted by several numerical wave predictions obtained at the coastal waters near Gunsan-Janghang Harbor. Field and numerical model investigations were initially conducted for the original navigation channel management project. We hope to contribute from this study that coastal engineers are able to use safely the numerical models in the area of port and navigational channel design.*

Key words : *Gunsan-Janghang Harbor, Spectral wave model, Energy balance model, Navigational channel design*

1. Introduction

Wave prediction considering wind growth and wave transformation path from offshore to nearshore with a very complicated coastal boundary is a critical component of most coastal engineering projects, e.g., management of navigational channel and designing or repairing coastal structures, especially at coastal inlets or beaches. These projects typically require a detailed knowledge of the wave field in the project area. However wave propagation is influenced by complex bathymetry, tide levels, winds, and wave generated currents. Therefore, the desired wave information is not readily available at the project site. Some information might be available from buoy observations or selected point measurements, usually at some considerable distance from the project area. On the basis of the sparse information, the coastal engineer is required to estimate the wave conditions at various situations.

Up to now the numerical simulation is more popular, cost effective, efficient, and rational tool for generating the desired estimation. Until recently, all coastal wave forecasts were made using a locally customized implementation of two major categories: models based on the conservation of energy and models based on the conservation of mass and momentum. However, energy balance models cannot incorporate the effects of diffraction and reflections caused by bathymetric features and structures. On the other hand, mass balance models cannot describe the effects of wind induced growth and the resulting wave-wave interaction. Vogel et al. (1988) described some important factors in this context.

Over the years, many researchers have developed models to describe the complex mechanisms such as refraction, diffraction, shoaling, breaking, friction, and reflection, etc. More recently, several versions of the third generation wave model have been implemented for the wind induced growth. The third generation model integrates using the spectral energy balance equation. Although there are rapid improvements on the numerical tools, the engineer taking in charge of a particular coastal project has no prior knowledge of which of these mechanisms is dominant or the result of the complex combination of various physical

* Corresponding Author : Joong-Woo Lee, jwlee@mail.hhu.ac.kr 051)410-4461
** seaprince1@hanmir.com 055)410-4981
*** vulcan98@hanmail.net 051)410-4981
**** minsuids@hotmail.com 051)410-4981
***** kikami@seil.com 02)840-5182

processes. It is beyond the realm of practical engineering or not possible to incorporate all physical processes with a single magic model, at present. Therefore, we should be prudent to use a model that can incorporate as many of these mechanisms as possible under the given environment.

Due to the special bathymetry of the Kunsan- Janghang tidal inlet, the waves off the western coast of Korea. As the large coastal reclamation work is going to be started near the inlet and navigation channel, it could cause coastal wave climate and unexpected changes to the waterways. We review some wave models that strive to provide an acceptable adaptation for the study area. The models described here are presently used for coastal projects. The following section summarizes the models with the governing equations to clarify the concepts behind various theories.

2. Description of Numerical Wave Model

2.1 Energy Balance Models

Energy balance models are generally used for the prediction of deep ocean wave climate. The well- known WAN3G model is based on a solution of the time-dependent energy balance equation for the complete range of discrete frequency and direction components that comprise the wave energy spectrum (WAMDI Group, 1988). A more recent development in this type of model called SWAN to retain all frequency components is done by Holthuijsen and Booij (1986). In SWAN the evolution of the wave spectrum is described by the spectral action balance equation which for Cartesian coordinates is as follows:

$$\frac{\partial N}{\partial t}+\frac{\partial c_X N}{\partial x}+\frac{\partial c_Y N}{\partial y}+\frac{\partial c_\sigma N}{\partial \sigma}+\frac{\partial c_\Theta N}{\partial \Theta}=\frac{S}{\sigma} \tag{1}$$

The first term in the left-hand side of this equation represents the local rate of change of action density (N) in time, the second and third term represent propagation of action in geographical space (with propagation velocities C_X and C_Y in $x-$ and $y-$ axis space, respectively). The forth term represents shifting of the relative frequency due to variations in depths and currents (with propagation velocity C_σ in $\sigma-$ space for frequency). The fifth term represents depth-induced and current-induced refraction (with propagation velocity C_Θ in $\Theta-$ space for direction). The expressions for these propagation speeds are taken from linear wave theory (Mei, 1983). The term $S(=S(\sigma,\Theta))$ at the right hand side of the action balance equation is the source term in terms of energy density representing the effects of generation, dissipation, and nonlinear wave-wave interactions. The corresponding source term for transfer of wind energy to the waves is commonly described as the sum of linear and exponential growth.

A comparable model which is the steady state spectral wave model, called STWAVE using F.D.M. scheme, has been developed by Resio (1981). This model is upgraded by the US Army Corps of Engineers and being evaluated (Smith, 2001). The governing equation for steady-state conservation of spectral wave action along a wave ray is given by (Jonsson, 1990):

$$\frac{\partial E}{\partial t}+(C_{ga})_i\frac{\partial}{\partial x_i}\frac{C_a C_{ga}\cos(\mu-\alpha)}{\omega_r}=\Sigma\frac{S}{\omega_r} \tag{2}$$

where, E = wave energy density divided by $(\rho_w g)$, ρ_w =density of water S =energy source and sink terms Interaction of waves with currents is considered in a reference frame moving with the current. Wave parameter in this frame are denoted with the subscript r for being "relative" to the current, and parameters in the non-moving reference frame are subscripted a for "absolute". The wave dispersion relationship is given in the moving reference frame as (Jonsson, 1990):

$$\omega_r^2=kg\tanh(kd) \tag{3}$$

where ω = angular frequency, g = gravitational acceleration, k = wave number, d = water depth.

Wave parameters in this frame are denoted with the subscript r for being "relative" to the current, and parameters in the non-moving reference frame are subscripted a for "absolute".

In the absolute frame of reference, the dispersion equation is:

$$\omega_a=\omega_r=kU\cos(\delta-\alpha) \tag{4}$$

where U = current speed, δ = direction of the current relative to a reference frame (the x-axis, here), α = wave orthogonal direction (normal to the wave crest).

$$C_a=C_r+U\cos(\delta-\alpha) \tag{5}$$

$$(C_{ga})_i=(C_{gr})_i+(U)_i \tag{6}$$

Solutions for refraction and shoaling also require wave celerity, C and group celerity, C_g , in both reference frames. STWAVE simulates depth-induced wave refraction and shoaling, current-induced refraction and shoaling, depth-and steepness-induced wave breaking, diffraction, wind-wave growth, and wave-wave interaction and whitecapping that redistri- bute and dissipate energy in a growing wave field.

2.2 Mass and Momentum Conservation Models

Models based on the conservation of mass and momentum are most widely used for predicting the shallow water wave climate considering the effects of varying coastal bathymetry and geometry and of coastal and harbor structures. Since the mild slope equation model after Berkhoff's derivation (1972) started for this regime, a lot of extensions and modifications have been made to include the additional mechanisms of wave transformation.

In order to model surface gravity waves in coastal area, it is well accepted to use the two-dimensional elliptic mild-slope wave equation. The basic equation may be written as follows:

$$\nabla \cdot (CC_g \nabla \hat{\eta}) + \frac{C_g}{C} \sigma^2 \hat{\eta} = 0 \qquad (7)$$

where $\hat{\eta}(x, y)$ is complex surface elevation function, from which the wave height can be estimated, σ=wave frequency under consideration (in radians/ second), C(x,y) = phase velocity = σ/k, $C_g(x,y)$ = group velocity= $\frac{\partial\sigma}{\partial k} = nC$ with $n = \frac{1}{2}\left(1 + \frac{2kd}{\sinh 2kd}\right)$, k(x,y)=wave number(=2π/L), related to the local depth d(x,y) through the linear dispersion relation: $\sigma^2 = gk \tanh(kd)$. Equation (7) simulates wave refraction, diffraction, and reflection in coastal domains of arbitrary shape.

From this derivation, Kirby (1984) modified and derived the following extension of the mild-slope equation that includes the effect of background currents:

$$\frac{D^2\Phi}{Dt^2} + (\nabla \cdot \vec{U})\frac{D\Phi}{Dt} - (CC_g \nabla\Phi) + (\sigma^2 - k^2 CC_g)\Phi + (\sigma^2 - \omega^2)\Phi = 0 \qquad (8)$$

where, the operator $\frac{D}{Dt} = \left(\frac{\partial}{\partial t} + \vec{U} \cdot \nabla\right)$, $\vec{U}(x, y) = (u, v)$ is the current field, and $\Phi(x, y, t)$ is the complex velocity potential at mean water surface. ($\Phi = \phi e^{-i\omega t}$, $\phi = ae^{-is}$)

This method has been successfully applied to various wave propagation situations in the context of finite difference model.

However, other mechanisms also influence the behavior of waves in a coastal area. The mild-slope equation can be extended as follows to include the effects of bottom friction and dissipation due to wave breaking.

$$\nabla \cdot (CC_g \nabla \hat{\eta}) + \left(\frac{C_g}{C}\sigma^2 + i\sigma w + iC_g \sigma \gamma\right)\hat{\eta} = 0 \qquad (9)$$

where w is the friction factor and γ is the wave breaking parameter. We have used the following form of the damping factor, following Dalrymple et al. (1984).

$$w = \left(\frac{2n\sigma}{k}\right)\left[\frac{2f_r}{3\pi}\frac{ak^2}{(2kd + \sinh 2kd)\sinh kd}\right] \qquad (10)$$

where $a (= H/2)$ is the wave amplitude and f_r is the friction coefficient. The friction coefficient depends on the Reynolds number and the bottom roughness. Typically, values for f_r are in the same range as for Manning's dissipation coefficient 'n', specified as a function of (x,y) assigning larger values for elements near harbor entrances to consider entrance loss. For the wave breaking parameter γ, we use the following formulation (Demirbilek, 1994).

$$\gamma = \frac{0.15}{d}\left(1 - \frac{0.16 d^2}{4a^2}\right) \qquad (11)$$

In addition to the above relationships, simulation of nonlinear waves may be conducted by using the mild slope equation. This is accomplished by incorporating amplitude-dependent wave dispersion, which has been shown to be important in certain situations. Equation (12) is rearranged to include the nonlinear dispersion relation.

$$\sigma^2 = gk[1 + (ka)^2 F_1 \tanh^5 kd]\tanh\{kd + kaF_2\} \qquad (12)$$

Where

$$F_1 = \frac{\cosh(4kd) - 2\tanh^2(kd)}{8\sinh^4(kd)}, \quad F_2 = \left(\frac{kd}{\sinh(kd)}\right)^4 \qquad (13)$$

A finite element model for coastal surface water wave with the extended mild slope equation, called CGWAVE, has recently found widespread use. The FE model is a general purpose, state-of-the-art wave prediction model. It is applicable to the estimation of wave fields in harbors, open coastal regions, coastal inlets, around islands, and around fixed or floating structures. While FE model simulates the combined effects of wave refraction-diffraction included in the basic mild-slope equation, it also includes the effects of wave dissipation by friction, breaking, nonlinear amplitude dispersion, and harbor entrance losses.

3. Model Setup and Input Conditions

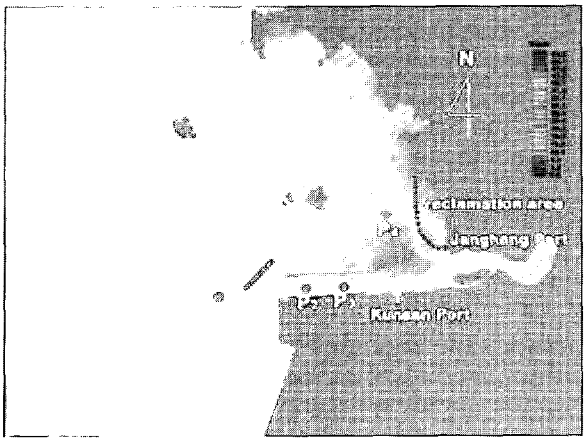

Fig. 1 Water depth at the model site

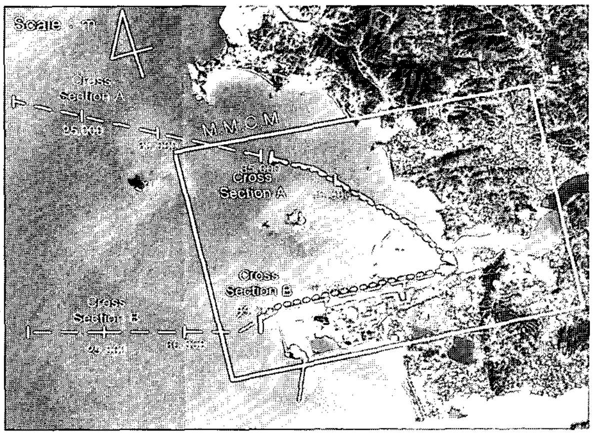

Fig. 2 Orientation of transect lines for the comparison of numerical simulation results

Kunsan-Janghang harbor have been developed continuously together with the plan of Kunsan coastal industrial zone formation which become a big portion of Korean coastal industries since 1970. The area has 4.6㎞ in total length of harbor line, 115 ㎢ in water dimension within the harbor, 5.5m~11m in the depth of water, and 7.24m in tidal range.

Kunsan-Janghang harbor is strategically important for international and domestic base industries because it is located near China. After construction of the new outer port, Kunsan-Janghang harbor would take a role of the most important port in the west coast of Korea. It also has Gum river at the mouth of the harbor, which brings a lot of sediment into the harbor. In this study, we tried to analyze and predict wave climate inside and outside the harbor to determine whether there are any significant differences between the two configuration set ups. The location and water depth of Kunsan-Janghang harbor are shown in Fig. 1. Fig. 2 shows the orientation of two transects and field stations for the comparison of numerical simulation and field mesurement results. The grids for F.D.M. models and meshes for F.E.M. model have shown in Fig. 3 and Fig. 4, respectively. P1 through P4 in Fig. 1 indicate stations for wave measurement for the period of one month at P2-4, and 7 months at P1.

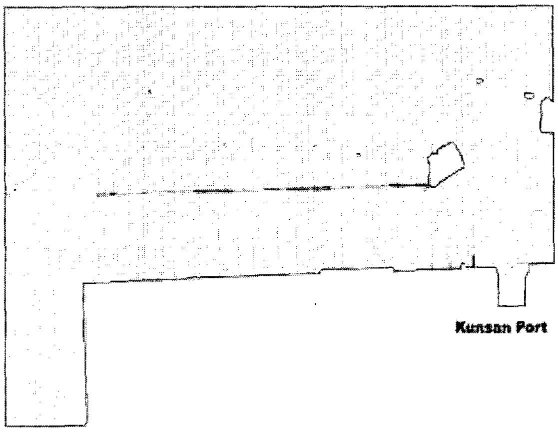

Fig. 3 Detailed mesh for F.D.M. at the site

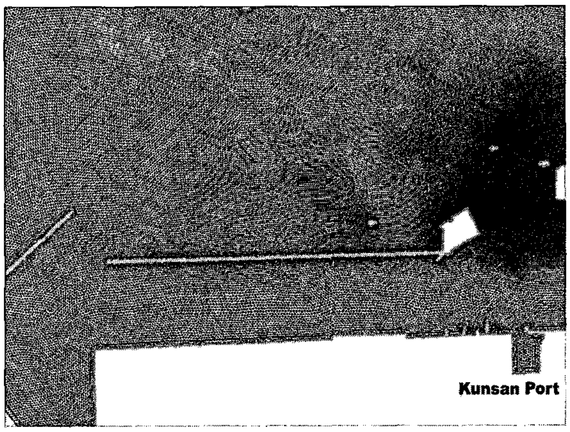

Fig. 4 Detailed mesh for F.E.M. at the site

Table 1 Incident wave condition for design wave

Direction	Height	Period	Return Period	Remark
W	4.2m	8 sec	50 year	MOMAF
WNW	5.0m	8.7 sec	50 year	MOMAF

Table 2 Numerical model characteristics

Case	Number of Nodes (Present/ After)	Calculation Time (P4, 3GHz)
F.D.M.(SWAN, STWAVE, PARANS)	63,000 / 63,000	56 min
F.E.M.	252,024 / 241,952	89 min

Table 3 Characteristics of wind

	Return Period	2 years	5 years	10 years	25 years	50 years	100 years
W	Wind Speed(m/s)	19.79	22.95	24.29	25.64	26.46	27.14
WNW	Wind Speed (m/s)	21.10	24.96	27.55	30.90	33.45	36.04

The deepwater design wave from WNW direction due to the winter trade wind, which impacts to Kunsan- Janghang harbor, is comparatively higher than that comes from SSW direction due to the summer typhoons. For numerical calculation of waves in this study, we set up those models described above with the incident wave parameters as shown in Table 1 and analyzed the result in terms of incident wave direction. Table 2 shows the required grid or node size for F.D.M. and F.E.M. For the present harbor it contains a total of 63,000 grids for F.D.M., 252,024 nodes for F.E.M., whereas for the reclamation configuration it covers a total of 63,000 grids for F.D.M. and 241,952 nodes for F.E.M. Table 3 shows the characteristics of wind of 26.46m/s (W) and 33.45m/s (WNW) (Korea Meteorological Administration, 2005). The site has a large tide. The tidal range of this area from the measurement (National Oceanogra- phic Research Institute, 2005) shows 624cm for spring tide, 275cm for neap tide and 450cm for mean tide. Tidal shape factor is 0.2, which means a predominantly semi-diurnal tide with two high waters and two low waters, alternatively.

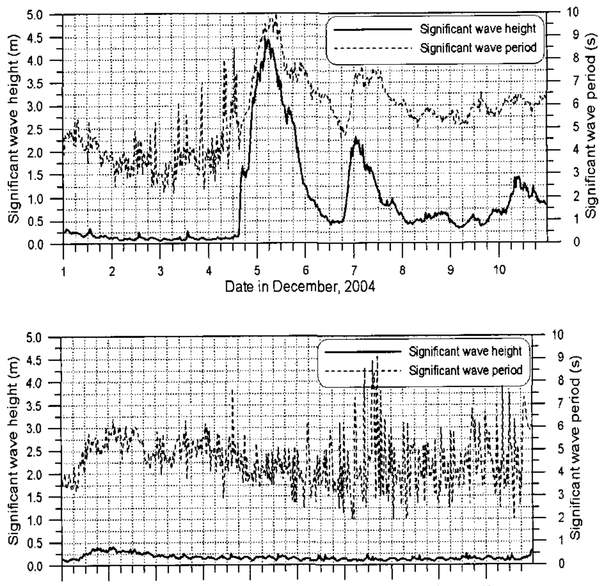

Fig. 5 The field measured significant wave heights (a) winter, (b) summer

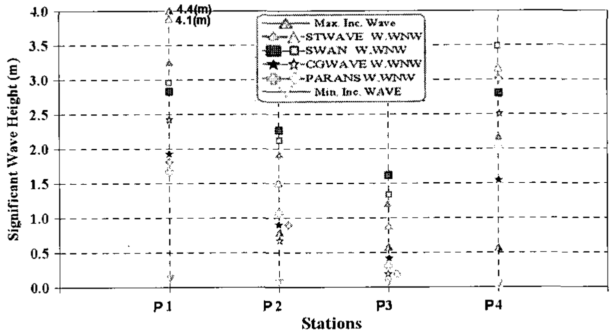

Fig. 6 Comparison with field measurement at the stations

4. Simulation Result and Analyses

Fig. 5 shows the field measured significant wave height in December, 2004 at P1. The maximum wave height reached 4.6m, which was the highest through the year. The data from numerical models at four stations are compared with the analyzed significant waves from field measurement in Fig. 6. The field data had shown pretty reasonable result with a numerical model during winter time. However, P2 through P4, inside harbor, the field data was slightly lower than the numerical models', because those were measured in summer time (June). Therefore, the predicted data from the models are slightly higher than the field data.

4.1 Result and Analyses by Energy Balance Model

Energy balance model can describe the effects of wind-induced growth and the resulting wave-wave interaction. Fig 7 and Fig. 8 are the pictures of predicted wave vector when wind comes from W. Fig. 9 and Fig. 8 show the predicted wave vector by SWAN when wind comes from W. When the wind effect, adopting 50 years return period, is considered, the waves penetrate inside of the harbor obviously.

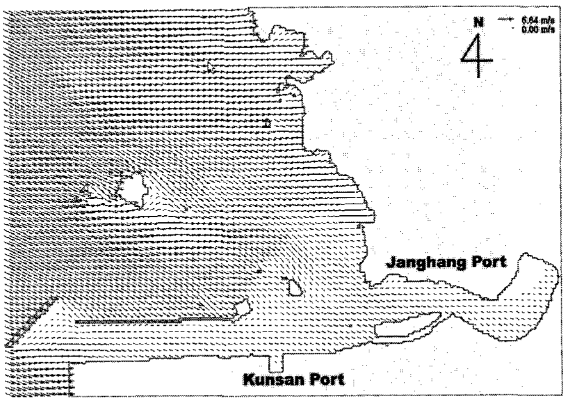

Fig. 7 Wave predictions by STWAVE for the present configuration with wave direction of W

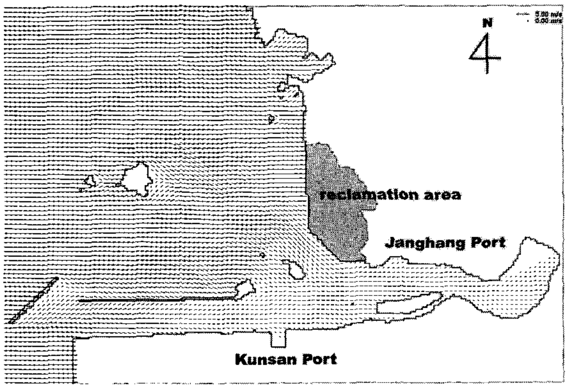

Fig. 8 Wave predictions by STWAVE for the new port configuration with wave direction of W

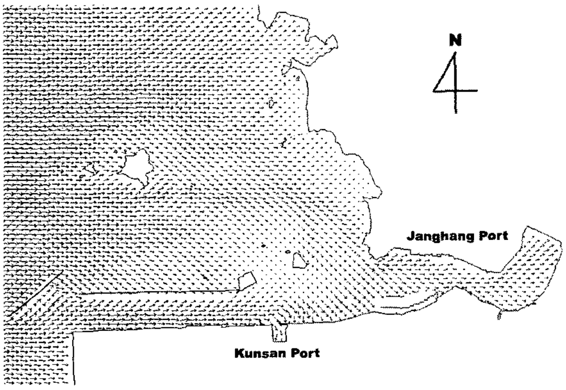

Fig. 9 Wave vector predictions by SWAN for the present configuration with wave direction of W

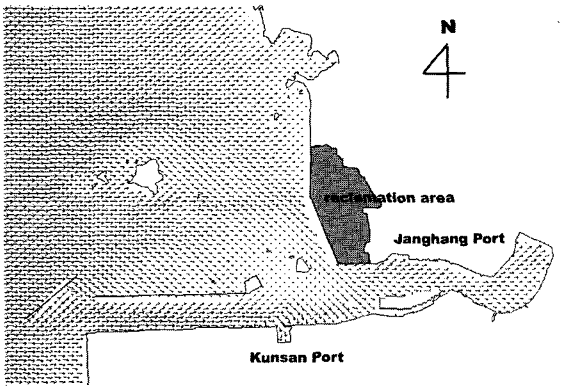

Fig. 10 Wave vector predictions by SWAN for the new port configuration with wave direction of W

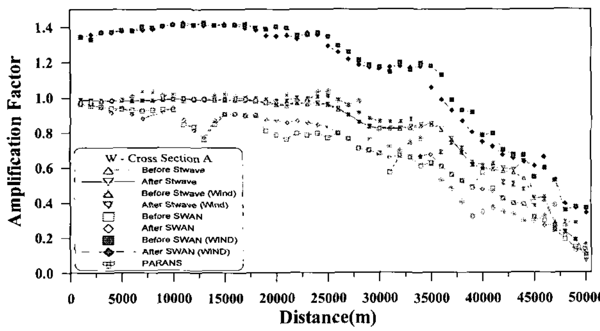

Fig. 11 Comparison of wave amplification factors along the cross section A (Wave direction W)

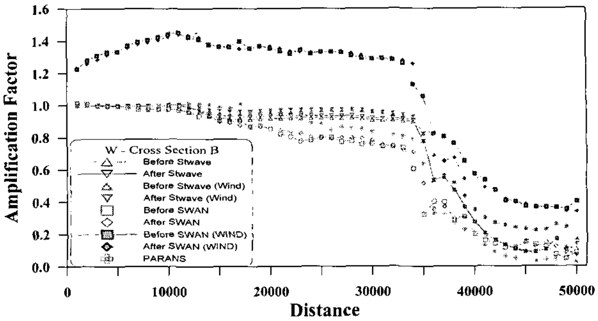

Fig. 12 Comparison of wave amplification factors along the cross section B (Wave direction W)

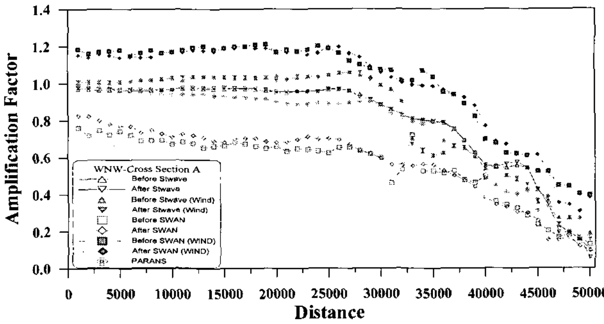

Fig. 13 Comparison of wave amplification factors along the cross section A (Wave direction WNW)

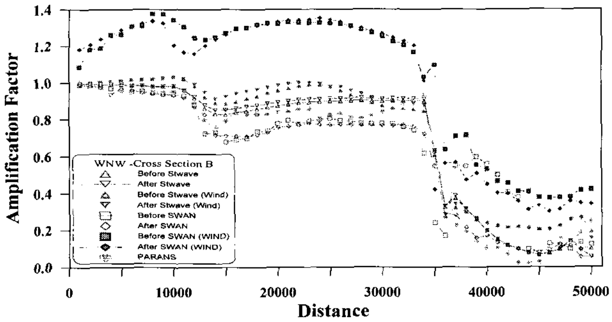

Fig. 14 Comparison of wave amplification factors along the cross section B (Wave direction WNW)

When the wind effect was considered, both models reveal the wind energy transmission effect showing that the wave amplification factors are slightly jumped by 0.2 to 0.4. It was more significant from the wave direction of W than WNW, because the waterway is exposed artificially and topographically to the wave direction of W. Fig. 11 through Fig. 14 are the comparison of wave amplification factors for present and after reclamation configuration along transect A and B, respectively. SWAN shows the highest results from any other models

The STWAVE shows a reasonable result comparing with the measurement data at the site. Fig. 11 shows that the amplification of the wave height decreases as it approaches to the harbor continuously. But in case of cross section B along the waterway in Fig. 10 where has constant water depth 10m to 12m by dredging and protection by the long breakwaters, the result shows the sudden drops of the wave amplification factors behind the detached breakwater at the leftmost.

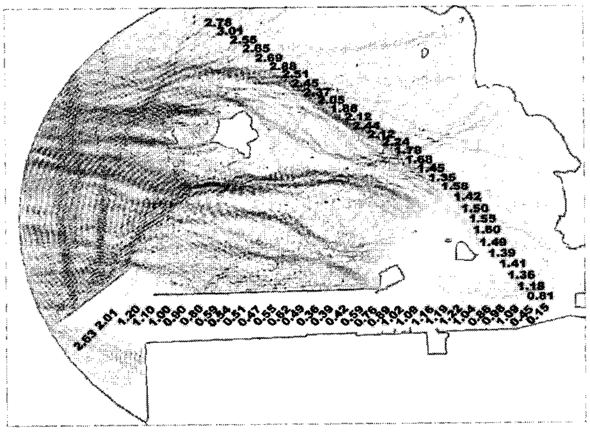

Fig. 15 Wave height predictions for the present configuration with wave direction of W

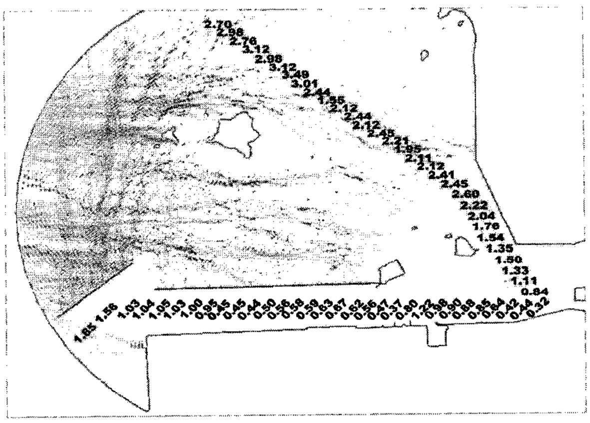

Fig. 16 Wave height predictions for after New port project with wave direction of W

4.2 Result and Analyses by Mass and Momentum Conservation Model

Mass and momentum conservation model can incorporate the effect of diffraction and reflections caused by bathymetric features and structures. Fig. 15 and Fig. 16 show the predicted wave height in case of present and new port configuration when waves come from W. As we can see the result in the figures, the reflected waves from the reclaimed area affect the wave field around Kunsan-Janghang port and its navigational channel as well. As we can see in Fig. 17 and Fig. 18, the wave amplification factors inside the harbor by mass and momentum conservation model are generally lower than that of the energy balance model.

It turned out that the wave amplification factors were increased about 15~20% at the Kunsan-Janghang port area due to the effect of diffraction and reflection considered by the models. It depends on wind effect or boundary reflection. Offshore island also causes some discrepancies. For this reason, therefore, we have to be careful when we make wave prediction on a certain site.

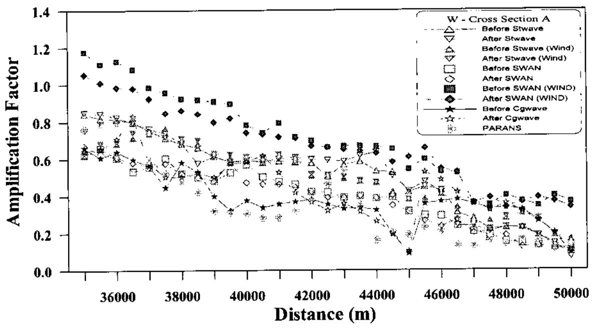

Fig. 17 Comparison of wave amplification factors along cross section A

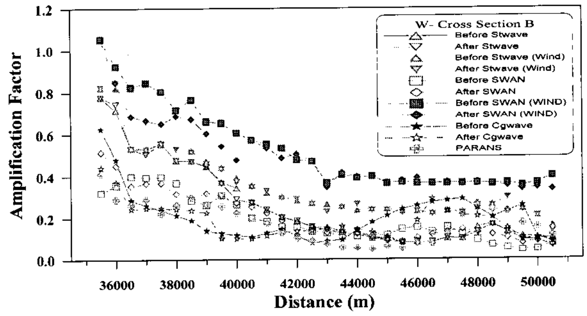

Fig. 18 Comparison of wave amplification factors along cross section B

5. Summary and Conclusions

We used four different numerical models for the present and new coastal configuration as an example to develop an understanding of the wave transformations that may be expected in such configurations. Although the field measurements for waves and currents in the area were not detailed enough for a systematic model validation, we think a general picture of wave climate were drawn.

The numerical results are sufficiently informative and all the statistics and line plots presented in this paper reason that those models are the excellent predicting tools and the produced results are agreed well with the physical basis. As no one model is the clear winner as per these comparisons, the selection of wave model should be followed after integral evaluation on the size and environment including depth and coastal shape of water domain, and the required calculation for precision and effectiveness.

For that reason, harbor design engineers should consider its economical and safety factors for the given area and situation by comparison of discrepanc- ies in every model.

References

[1] Berkhoff, J. C. W. (1972), "Computation of Combined Refraction-Diffraction," Proc. 13th Int. Confer. Coastal Engineering, ASCE, Vancouver, Canada, Vol. 1, pp. 471-490.

[2] Dalrymple, R. A., Kirby, J. T., and Hwang, P. A. (1984), "Wave Diffraction due to areas of high energy dissipation," J. Waterway, Port, Coastal and Ocean Eng., Vol. 110, pp.67-79.

[3] Demirbilek, Z. (1994), Comparison between REFDIFS and CERC Shoal Laboratory Study, Unpublished Report, Waterways Exp. Station, Vicksburg, MS.

[4] Holthuijsen, L. H. and Booij, N. (1986), "A Grid Model for Shallow Water Waves," Proc. 20th Int. Conf. Coastal Engineering, Taipei, Taiwan, pp. 261-270.

[5] Jonsson, I. G. (1990), "Wave-current interactions," The sea, Vol. 9, Part A, B (ed. B. Le Mehaute and D.M. Hanes), John Wiley & Sons, Inc., New York.

[6] Kirby, J. T. & R. A. Dalrymple (1984), "Verification of a Parabolic Equation for Propagation of Weakly-Nonlinear Waves," Coastal Engineering, Vol. 8, pp. 219-232.

[7] Korea Meteorological Administration (2005), Climate Information.

[8] Mei, C. C. (1983), The Applied Dynamics of Ocean Surface Waves, John Wiley, New York.

[9] National Oceanographic Research Institute (2005), Ocean Data: Real Time Coast Data.

[10] Resio, D. and W. Perrie (1991), "A numerical study of nonlinear energy fluxes due to wave-wave interactions, Part 1: Methodology and basic results," J. Fluid Mech., Vol. 223, pp. 609-629.

[11] Smith, J. M. (2001), "Modeling nearshore transformation with STWAVE," Coastal and Hydraulics Engineering Technical Note CHETN I-64, US Army Engineer Research and Development Center, Cicksburg, MS.

[12] Vogel, J. A., Radder, A.C., and de Reus, J. H. (1988), "Verification of Numerical Wave Propagation Models in Tidal Inlets," Proc. 21st. Int. Coastal ngineering Conference ASCE, Malaga, Spain.

[13] WAMDI Group (1988), "The WAM Model - A Third Generation Ocean Wave Prediction Model," J. Phys. Ocean., Vol. 18, No. 12, pp. 1775-1810.

Received 12 September 2005
Accepted 29 September 2005